Disorder effect on electronic and optical properties of doped carbon nanotubes

Jun Ma,[1] Shuguang Guan,[1,*] and C.-H. Lai[2]
[1]*Temasek Laboratories, National University of Singapore, 5 Sports Drive 2, 117508 Singapore*
[2]*Department of Physics, National University of Singapore, 117543 Singapore*
(Received 9 May 2006; published 1 November 2006)

In this work, we investigate the effects of disorder in the doped carbon nanotubes. Based on the extended Su-Schrieffer-Heeger model, it is shown that with the increase of doped impurity atoms, such as nitrogen or boron, the symmetry of the hopping processes among the doped and carbon lattices collapses, and the statistics of the nearest neighbor energy level spacing changes from the Poisson distribution to the Wigner distribution, indicating the occurrence of disorder effect in heavily doped nanotubes. As a result, the nanotube changes from a metal to a semiconductor. We also study the disorder effect on linear optical absorption in doped nanotubes. It is demonstrated that the linear optical absorption can be greatly suppressed due to the collapse of the discrete spatial symmetry in heavily doped nanotubes. Based on the random matrix theory, we carry out a theoretical analysis, which agrees well with our numerical simulations.

DOI: 10.1103/PhysRevB.74.205401 PACS number(s): 05.45.−a, 72.80.Rj, 33.15.−e

I. INTRODUCTION

Recent years have witnessed increasing interest in the study of complicated many-particle systems, including nuclei, atoms, molecules, quantum chaotic, and disordered systems. A great variety of numerical and experimental works have shown Wigner level statistics, random matrix ensembles, wave function scars, and other dynamical features.[1–13] These researches not only reveal deep physical insights in the microscopic and mesoscopic worlds, but also have significant impact on the developments in nanotechnology.

As new generation materials, fullerenes and carbon nanotubes have attracted much research attention since they can exhibit semiconductor, metal, or insulator properties depending on their diameters and other geometric structures.[14] Fullerenes and carbon nanotubes have great potential in various applications in electric circuits and optical devices. For example, experiments indicate that nanotubes can even be used as an atomic-scale pinning material in high-T_c superconductor. One important and effective method to change the properties of fullerenes and carbon nanotubes is to dope them with impurity atoms. During the last decade, such techniques have been successfully developed,[15,16] and subsequently, the structural, electronic, and optical properties of doped fullerenes and carbon nanotubes have been intensively investigated.[17–19] There are two doping approaches; one is to capture the alkali metal atoms in the fullerenes or nanotube cage; the other is to substitute some carbon atoms of fullerenes or nanotube by the impurity atoms such as nitrogen or boron atoms.[20] In the latter case, since the delocalized electrons in the pure fullerene or nanotube become localized around the doped atoms,[17] the distribution of electrons in doped fullerene or nanotube changes accordingly. Therefore, the structural and electronic properties of doped fullerenes or nanotubes can be significantly altered. For example, it is found that the energy gap could vary dramatically by even doping one impurity atom into C_{60}.[17] This implies that one could conveniently change a metallic fullerene or nanotube to an insulator fullerene or nanotube, or vice versa.

For an infinitely long nanotube, the symmetries of translation, reflection and rotation are preserved. Due to these high geometric symmetries, we believe that the energy spectrum of pure carbon nanotubes satisfies the Poisson statistics. Similarly, in slightly doped nanotubes, it is not likely for total disorder effect to occur since the partial symmetries in the system can still be preserved. This argument is supported by previous studies on slightly doped C_{60},[17] which shows that relatively high degeneracy still exists in such systems. With technical progress, it is now possible to dope many impurity atoms in a carbon nanotube. With sufficient impurity atoms, it can be imagined that the doped nanotube will completely lose its geometric symmetries. Obviously, heavy doping will lead to disorder effect in the fullerenes and nanotubes. Naturally there are two questions to be explored. One is how to characterize this disorder effect, and the other is how the doping affects the physical properties of fullerenes or nanotubes. In the present work, we answer these questions by characterizing the disorder effect in doped carbon nanotubes and further studying its effects on the electronic and optical properties of doped nanotubes.

On the other hand, it has been shown that the dynamics of electrons in a random impurity potential relates to the phenomenon of quantum chaos. In a zero-dimensional nonlinear σ model, Efetov confirmed the conjecture that weakly disordered metal follows the same statistics as random ensembles.[21–23] In this paper, the system we study is the electron moving in a random potential with lattice distortions, which means the electron collides not only with impurities but also with the lattices and their distortions caused by impurities. Therefore, we expect that similar and new properties could show up in doped carbon tubes.

Based on the Su-Schrieffer-Heeger (SSH) model, we calculate the energy spectrum for doped nanotubes. It is found that with the increase of doped impurity atoms, the statistics of the energy level spacings changes from the Poisson distribution to the Wigner distribution, which characterizes the occurrence of disorder in heavily doped nanotubes. Moreover, the signatures of disorder effect have also been characterized in terms of the eigen wave functions and the distribution of the excess charges in the system. We further

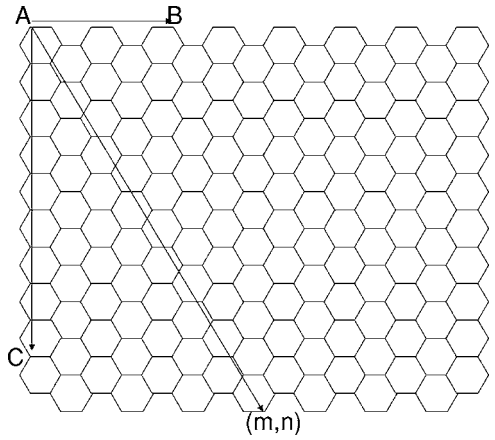

FIG. 1. The structures of a nanotube. Rolling up this sheet and joining the points A and B, an armchair nanotube could be obtained, and joining the points A and C, a zigzag nanotube could be obtained. The vector (m,n) between the two joined points determines the diameter and tip of the nanotube.

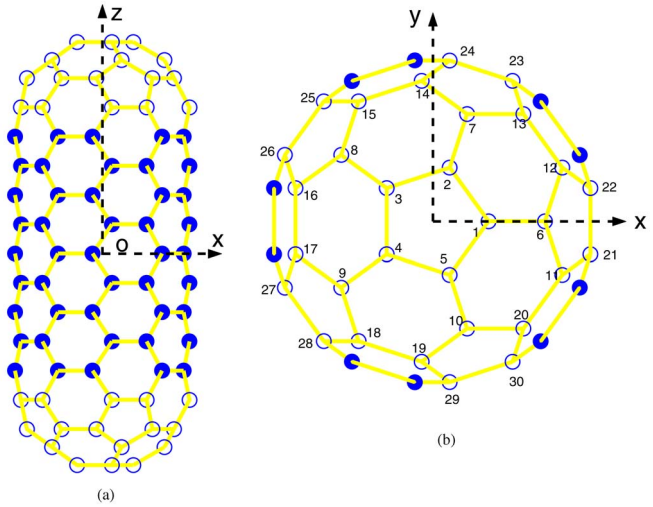

FIG. 2. (Color online) The architecture of armchair nanotube in the (a) xz plane and (b) xy plane. The total atoms in the shown picture are 150, and the space circle denotes the atoms on the caps. The numbering rule is as follows: we consider the atoms with the same z as in the same level; the numbering starts from the toppest level; at each level the numbering goes counterclockwise as shown in the figure.

investigate the disorder effect on the optical properties of doped nanotubes. It is found that the optical absorption can be significantly suppressed in the disorder regime. Based on the random matrix theory, a theoretical analysis is present which agrees well with our numerical observations.

The organization of this paper is as follows. In Sec. II, a theoretical model for doped carbon nanotubes is described. Section III investigates the electronic structures and the statistics of eigen wave functions for the doped nanotubes. Section IV is devoted to the disorder effect on optical properties of doped carbon nanotubes. The conclusion is given in last section.

II. THEORETICAL MODEL

Cylindrical carbon nanotubes can be fabricated by rolling a two-dimensional graphite honeycomb lattice. The geometrical structure of a nanotube is uniquely determined by a set of vectors. The honeycomb lattices can be labeled by the vector $\mathbf{R}=m\mathbf{a}+n\mathbf{b}$, where $\mathbf{a}$ and $\mathbf{b}$ are the lattice translation vectors on the graphite sheet, and m,n are integers (see Fig. 1). The pair of numbers (m,n) define the radius and chirality of the nanotube. The tips of the nanotubes might be very complicated; therefore, most nanotubes do not have caps. Two typical types of self-consistent nanotubes with closed caps are the armchair [see Fig. 2(a)] and zigzag nanotubes, which actually are the molecules C_{60+10j} and C_{60+18j}, respectively. The caps can be obtained by cutting a C_{60} molecule into two halves along its equatorial line, as shown in Fig. 2(b). The length of the nanotube increases linearly with the integer j. Theoretically, one can construct an infinitely long nanotube by increasing j. In the present work, we choose the armchair nanotube as the object to investigate the disorder effects on the electronic and optical properties in doped nanotube. We believe that the doping effects are essentially the same for both the armchair and the zigzag nanotubes.

It is known that the electron-phonon interaction plays an important role in one-dimensional carbon chain such as polyacetylene. This interaction leads to an energy gap and instability, which transform a metallic chain into an insulated chain due to dimerization. Therefore, the bonds in polyacetylene can be divided into two kinds, i.e., the long σ bond and the short π bond. It is pointed out that at least these two kinds of bonds exist in carbon nanotubes as well. The long bond includes two electrons and the short bond includes only one electron. This indicates that dimerization happens in a nanotube and will greatly affect its electronic structure. To describe the electron in the doped nanotube with the electron-phonon interaction, an appropriate model is the extended SSH model,[14,17,18] which has the total Hamiltonian as

$$H = \sum_{\langle ij\rangle,s} [-t_{ij} - \alpha_{ij}(u_i^j + u_j^i)](c_{i,s}^\dagger c_{j,s} + c_{j,s}c_{i,s}^\dagger) + \frac{1}{2}K_{ij}\sum_{\langle ij\rangle}(u_i^j + u_j^i)^2, \quad (1)$$

where t_{ij} is the hopping integral of the system with the uniform bond length; α_{ij} the electron-phonon coupling; and K_{ij} the spring constant. Since the nanotube has been doped, there are three sets of parameters for $(t_{ij},\alpha_{ij},K_{ij})$, i.e., (t_0,α_0,K_0) for the C-C bonds, (t_1,α_1,K_1) for the C-X bonds, and (t_2,α_2,K_2) for the X-X bonds. Here X denotes the doped impurity atom. The operator $c_{i,s}^\dagger$ creates a π electron at the ith atom with spin s, u_i^j is the displacement of the ith atom from the jth atom, and the sum is taken over the nearest neighbor pairs of $\langle ij\rangle$. The term $(u_i^j+u_j^i)$ denotes the change of length of the bond between the ith and jth atoms. The second term in Eq. (1) represents the elastic energy of the phonon system.

TABLE I. The parameters t, α, and K for different bonds in the present computation.

Bond	t (eV)	α (eV/Å)	K (eV/Å)
C-C	2.5	6.31	49.7
C-B	0.81	5.8	53
B-B	0.9	5.0	58
C-N	1.4	6.0	46
N-N	0.79	3.0	43

Equation (1) can be solved by the adiabatic approximation for the phonon.[14,17,18] The eigenstate equations for the π electrons are

$$\epsilon_k \phi_{k,s}(i) = \sum_{\langle ij \rangle} [-t_{ij} - \alpha_{ij}(u_i^j + u_j^i)]\phi_{k,s}(j), \tag{2}$$

where ϵ_k is the eigenvalue of the kth eigenstate. The self-consistent equations for $(u_i^j + u_j^i)$ can be derived as

$$u_i^j + u_j^i = \frac{2\alpha}{K} \sum_{k,s}{}' \phi_{k,s}(i)\phi_{k,s}(j) - \frac{2\alpha}{K}\frac{1}{N_b}\sum_{\langle kl \rangle}\sum_{m,s}{}' \phi_{m,s}(k)\phi_{m,s}(l), \tag{3}$$

by minimizing the total energy $E(u_i^j + u_j^i)$ and using the constrain condition

$$\sum_{\langle ij \rangle} (u_i^j + u_j^i) = 0. \tag{4}$$

Here the prime in Eq. (3) denotes that the sum is taken over the occupied states, and N_b is the number of the π bond which equals to $(90+15j)$ for armchair nanotubes.

For the SSH model, the parameters (t_{ij}, α_{ij}, K_{ij}, $ij=0,1,2$) are important because they represent the microscopic interactions inside the nanotubes. It is desirable to determine these parameters by experiments. Unfortunately, such experiments are generally not available nowadays. Based on studies of pure C_{60}, the parameters (α_0, K_0, t_0) can be taken as $t_0=2.5$ eV, $\alpha_0=6.31$ eV/Å, and $K_0=49.7$ eV/Å.[19] Since except for nearest neighbor lattice, doped atoms have little influence on other long-range bonds, all original parameters for pure C_{60} can be retained for the carbon-carbon bonds in doped fullerenes. In order to include the effect of doped atoms, parameters (t_{ij}, α_{ij}, K_{ij}, $ij=1,2$) should be adjusted for the undimerized system. Numerically, we carefully adjust these parameters so that our calculation based on these parameters can accurately reproduce the results obtained from SCF-MO method.[24,25] The parameters used in this study are listed in Table I. In Table II, our numerical results of the energy gaps between the highest-occupied molecular orbital (HOMO) and lowest-unoccupied molecular orbital (LUMO) are compared with those obtained by the SCF-MO method.

TABLE II. The energy gaps (in eV) between the LUMO and the HOMO for doped C_{60} using SCF-MO method and SSH method with the parameters in Table I.

	$C_{59}B$ (1)	$C_{58}B_2$ (1,2)	$C_{59}N$ (1)	$C_{58}N_2$ (1,2)
$\Delta\epsilon$ (SCF-MO)	1.06	0.49	0.30	0.23
$\Delta\epsilon$ (SSH)	1.06	0.49	0.30	0.23

III. THE SIGNATURES OF SPECTRUM OF RANDOM MATRIX ENSEMBLES

It is known that a pure long armchair nanotube has very high geometric symmetry. Besides the fivefold rotational symmetry, it also has the longitudinal shift symmetry. Therefore, a long pure armchair nanotube should be metallic, i.e., the energy gap between the HOMO and the LUMO should approach zero as the nanotube becomes infinitely long.[14] However, the geometric symmetries are discrete and could not be described by any continuous parameter, so there does not exist any explicitly conserved dynamical variable. But the whole structure of hopping integrals between the nearest neighbor lattices is determined by those discrete spatial symmetries, which allow the Hamiltonian matrix to be constructed directly. As a consequence, the Hamiltonian matrix has very high symmetry among its elements, which suggests that the statistics of level spacings could be a Poisson distribution.

However, the method to measure the disorder effect in the electronic structures is a problem. In contrast to a pure nanotube, each eigenstate of heavily doped systems is characterized only by its energy rather than by a set of degeneracy, which reminds us the analysis of atomic nuclei[26,27] and complex molecules.[28] Haq, Pandey, and Bohigas examined various elementary statistics of spectra of complex nuclei and found the level spacing distribution and spectral rigidity are identical to those resulting from random matrix theory.[27] Their success convinces us that random matrix theory is an important tool to describe the disorder effect in nanotubes as well. In this paper, we focus on comparing the level spacing distribution and level number variance with random matrix ensemble. If the comparison indicates random matrix theory is fulfilled, the heavily doped nanotubes could be treated within a statistical framework subsequently. Therefore, basing on the statistical characteristic of random matrix ensembles, we could analytically figure out new properties of electronic structure and optical absorption.

We first compute the electronic structures of an armchair nanotube with $j=15$ doped by 1, 2, or 3 nitrogen atoms, respectively. Their electronic structures near the HOMO and the LUMO are shown in Fig. 3. Theoretically a long armchair nanotube is metallic,[14] i.e., its energy gap should be less than 0.1 eV. As shown in Fig. 3, when one nitrogen atom is doped, the energy gap between the LUMO and the HOMO has already risen to 0.2 eV; when three nitrogen atoms are doped, the energy gap increases to 0.35 eV, indicating that this doped nanotube is already a semiconductor. In addition, the doping can reduce the degenerate levels in the electronic structure. For example, the highest level shown in

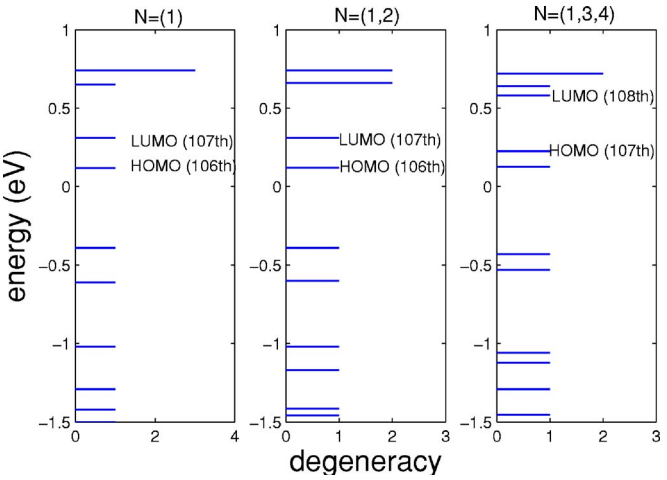

FIG. 3. (Color online) The energy level structures of slightly doped nanotubes. The total atoms are 210. If the difference between two levels is less than 0.02 eV, they are considered as degenerate. The numbers in the bracket denote the positions of the doped atoms.

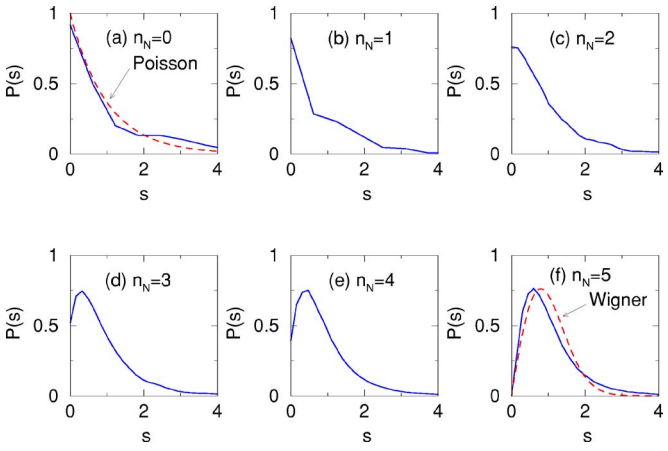

FIG. 4. (Color online) The distribution of the energy level spacing $P(s)$ for nitrogen-doped armchair nanotubes. $P(s)$ is obtained by ensemble average of randomly distributed doped atoms. n_N is the numbers of doped nitrogen atoms. The total atoms are 210.

the left panel in Fig. 3 has a threefold degeneracy, but in the middle panel, there are only two twofold degenerate levels. With three doped nitrogen atoms, one of the two twofold degenerate levels further becomes nondegenerate. This clearly demonstrates that the more the impurity atoms are added, the lower the degeneracy of the electronic energy spectrum. As shown in Fig. 3, the doping could destroy the geometric symmetry of pure nanotube and thus change its electronic structure. It can be imagined that with the increase of the doped impurity atoms, the geometric symmetry of a pure nanotube will be gradually destroyed and the disorder effect can be expected to occur after that.

We now look for the signatures of disorder effect in doped armchair nanotubes. It has been shown that there exists a remarkable universality in the spectral correlations of complicated of systems. Usually, the statistics of the nearest neighbor spacing turns out to be a good measure to characterize the disorder. For regular systems, the nearest neighbor energy level spacings follow the Poisson distribution

$$P^P(s) = \exp(-s), \tag{5}$$

where s represents the nearest neighbor energy level spacing. On the other hand, in the disordered or chaotic systems, the distribution of the nearest neighbor energy level spacings satisfy the Wigner distribution

$$P^W(s) = \frac{\pi}{2} s \exp\left(-\frac{\pi}{4} s^2\right). \tag{6}$$

In order to find whether the energy spectrum of a nanotube is regular or disordered, we can use two criteria, i.e., Eqs. (5) and (6), as empirical measures. To this end, we compute the distributions of the nearest neighbor energy level spacings for different configurations of the nanotubes, including pure nanotubes and doped nanotubes with increasing numbers of doped nitrogen atoms from 1 to 5. The results are shown in Fig. 4. Figure 4(a) is for the pure nanotube, which resembles the Poisson distribution. It should be pointed out that in the extended SSH model for the pure nanotube, there are no conserved dynamical variables as in an integrable system. However, the results still preserve the characteristics of a regular spectrum due to its high geometric symmetry. In Figs. 4(b)–4(e), with the increase of the doped nitrogen atoms, the energy level spacing statistics gradually deviates from the Poisson distribution. The longer tails there remind us of the Brody distribution.[3] Finally, in Fig. 4(f), with five doped nitrogen atoms (2.4% of the total atoms), the distribution of the nearest neighbor energy level spacings roughly reaches the Wigner distribution. With further increase of the doped impurity atoms, the energy level spacing statistics further approaches the Wigner distribution, as shown in Fig. 5(a). The situation is basically the same when boron atoms are doped. As shown in Fig. 5(b), only 5 boron atoms (1.6% of the total atoms) generate a Wigner-like spectrum approximately, and with ten doped boron atoms the distribution further approaches the Wigner distribution. We systematically investigated the doping effect on the statistics of the energy level spacings for nanotubes from j=9 to 95 (j is chosen as odd number in the present study). The results are similar to those shown in Figs. 4–7. Usually, a few percent of impurity atoms are enough to lead to a Wigner-like energy level spacing distribution, which characterizes a completely disorder

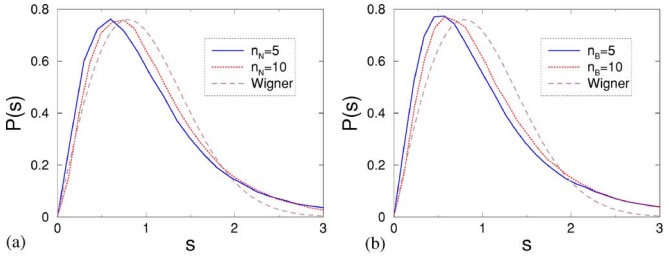

FIG. 5. (Color online) The distribution of the energy level spacing $P(s)$ for nitrogen-doped armchair nanotubes. $P(s)$ is obtained by ensemble average of randomly distributed doped atoms. n_N and n_B are the numbers of doped nitrogen and boron atoms, respectively. (a) The total atoms are 210. (b) The total atoms are 310.

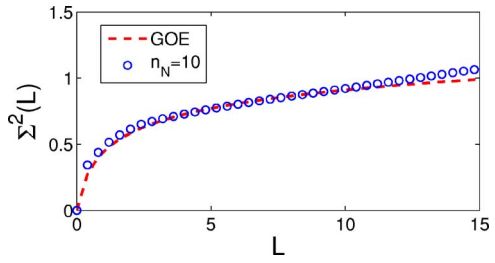

FIG. 6. (Color online) Level number variance $\Sigma^2(L)$ for the doped carbon nanotubes and GOE. The total atoms are 510. n_N is the numbers of doped nitrogen atoms. The results are obtained by ensemble average.

regime in doped nanotubes. It is known that the Wigner distribution implies level repulsion, which makes the doped nanotube a semiconductor. On an average, the energy gap of the doped nanotubes between the HOMO and the LUMO is the mean level spacing, which is much larger than that of the pure nanotube since the pure one has almost zero energy gap due to high degeneracy of energy level and is thus metallic. In certain one-dimensional nanosystems, the impurity usually causes the metal-insulator transition. Here, our analysis shows the disorder effect due to doping would statistically lead to the metal-semiconductor transition in nanotubes. It should be emphasized that this conclusion is based on the statistics. The Wigner distribution does not rule out the slight possibility that the individual nanotube with many impurities has small energy gap.

However, the transition from the Poisson distribution to the Wigner one does not display the characteristic in large scale since the nearest neighbor level spacing is certainly to study the short energy scale. It is well known that the Thouless energy is an important measure to probe the large scales of spectrum. Especially, in the disordered mesoscopic systems, a dimensionless conductance equals the average number of level within the Thouless energy $E_c = \hbar D/L^2$, where D is the diffusion constant and L is the size of samples.[22,23] Spectral rigidity consistent with strong level repulsion could be related to dimensionless conductance. This reminds us to study the spectral rigidity or level number variance. As an example, the level number variance for a doped nanotube

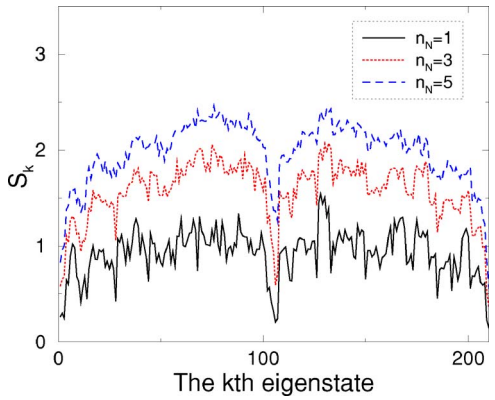

FIG. 7. (Color online) The entropy (in H_0 representation) vs eigenstate. The total atoms are 210. The results are obtained by ensemble average.

with totally 510 atoms is plotted in Fig. 6, where the Thouless energy could be read off. The starting point of deviation between two lines indicates a small Thouless energy, which implies that in the doped nanotubes, the number of energy levels within the Thouless energy is also small, and so is the dimensionless conductance.

Another frequently used criterion for disorder effect is the entropy based on the eigen wave functions. Assuming the doped atoms as a perturbation V, we rewrite the Hamiltonian for the doped nanotube as

$$H = H_0 + V, \tag{7}$$

where H and H_0 are Hamiltonians for the doped and pure nanotubes, respectively. First, the eigen wave functions of a pure nanotube is computed and used as basis; then the eigen wave functions of H for the doped system are expanded in this basis. To measure how disordered the eigen wave functions are, the entropies can be calculated as

$$S_m = -\sum_n |\langle \psi_m | \psi_n^0 \rangle|^2 \ln |\langle \psi_m | \psi_n^0 \rangle|^2, \tag{8}$$

where $|\psi_m\rangle$ and $|\psi_n^0\rangle$ are eigen wave functions of the doped and pure systems, respectively. In Fig. 7, an example is shown for $j=15$ nanotube with 1, 3, or 5 doped nitrogen atoms. It is found that the more the impurity atoms, the larger the entropy of the eigen wave functions. In the case of five doped atoms, the entropy almost reaches 3. This indicates that the eigen wave functions have sufficiently extended in the H_0 representation, which characterizes the occurrence of disorder effect.

For the extended SSH model, the excess charge could also be conveniently computed, which can be used as an indicator for disorder in doped nanotubes. The advantage of this characterization is that it can be observed in experiments. The excess charge at the ith lattice is defined as[17]

$$Q_i = \sum_{m,s}{}' \psi_{m,s}^*(i)\psi_{m,s}(i) - 1. \tag{9}$$

In Fig. 4(c), it is shown that the spectrum for the nanotube with two doped atoms approximately retain the characteristics of the Poisson distribution. Furthermore, in the middle panel of Fig. 3, partial degeneracy of the energy levels still exists. These indicate that the excess charge may preserve some structures in slightly doped nanotubes. This argument can be justified by our numerical experiment. For $j=15$ nanotube, totally there are 210 carbon atoms including the caps. We substitute two nitrogen atoms at the middle lattices 105 and 106 (see Fig. 2 for the numbering of lattices). In this way, the doped armchair nanotube still has partial rotation and reflection symmetries. This requires that the excess charge distribution should also respect the same symmetries. In Fig. 8(a), the distribution of the excess charge for the doped nanotube is plotted, and its symmetry is evident. For instance, the excess charges at lattices 105 and 106 are the same, i.e., $-0.0128e$. This is reasonable since the two doped nitrogen atoms are totally equivalent. In Fig. 8(b), two distributions are shown for two different nanotubes in the disorder regime. For the disordered nanotube without caps, sto-

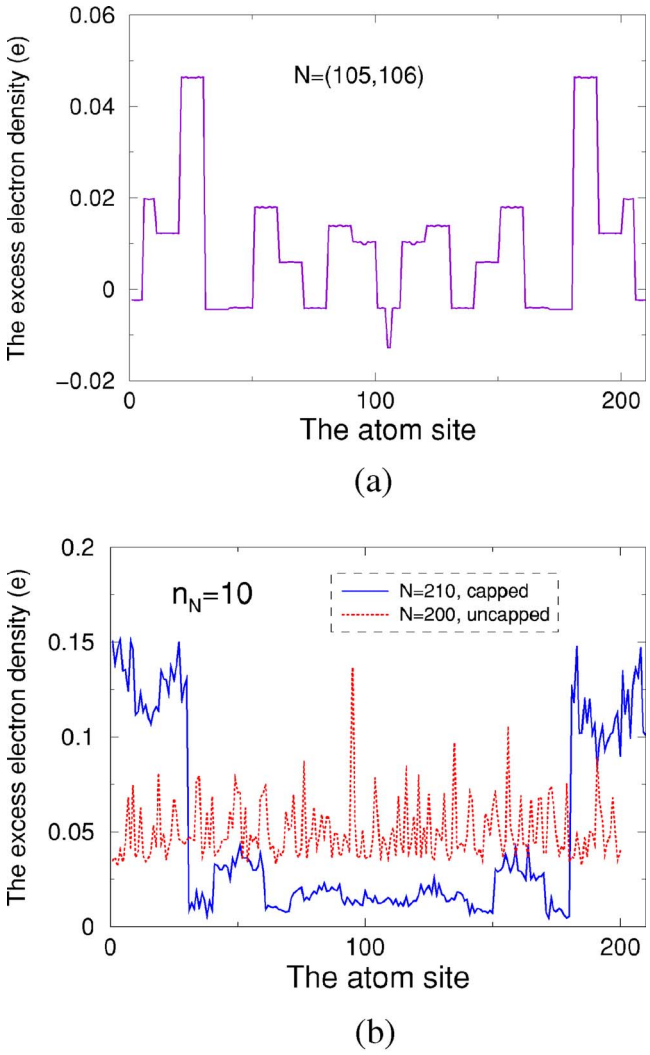

FIG. 8. (Color online) The distribution of the excess electron charge density. (a) Two doped nitrogen atoms are at lattices 105 and 106, respectively. The total excess electron density is $2e$. The distribution of the excess electron charge bears the reflectional symmetry of the system. (b) Ten doped nitrogen atoms are randomly distributed. The total excess electron charge is $10e$. The results are obtained by taking ensemble average.

chastic distribution of the excess charge is observed as expected. However, the distribution of the excess charge in a disordered nanotube with caps is not stochastic. Instead, surprisingly, the most excess charges are found to be localized around the two caps. This is somehow beyond our expectation. We attribute this phenomenon as the cap effect which actually is a kind of boundary effect. Hopefully, such effect might be useful for designing new devices in practice.

IV. DISORDER EFFECT ON OPTICAL ABSORPTION

Apart from the signatures of disorder in the distributions of the energy level spacings and eigen wave functions discussed in the previous section, optical absorption provides another very important indicator of disorder since it is experimentally accessible. So far, the optical response of fullerenes has been investigated by many experimental techniques, such as the degenerate four-wave mixing, the third-harmonic generation, the electric-field-induced second harmonic generation, and so on.[29,30] It has been observed that the linear optical absorptions of C_{60} and C_{70} are less than 10^{-20} esu,[31–33] which are of the same order as that for quasi-one-dimensional conducting polymers. On the one hand, the residual infrared absorption of the linear conjugated polymers caused by the overtones of carbon-hydrogen bond vibrations prevents their applications in photonic communications.[33] On the other hand, the absence of carbon-hydrogen bonds promises that the pure or doped nanotubes are potential candidate materials for designing devices in optical communications. Therefore, either from a theoretical or an experimental viewpoint, it is necessary to investigate how the disorder induced by doping affects the optical properties in nanotubes.

The optical absorption of nanotubes can be calculated by the following formula:[17]

$$\alpha(\omega) = \sum_{b,a} \mu_{b,a}^2 \delta(\hbar\omega + \epsilon_a - \epsilon_b), \tag{10}$$

where $\mu_{b,a}$ is the dipole transition matrix between molecular orbitals ψ_b and ψ_a, which can be expressed as

$$\langle b|\mu_r|a\rangle = \sum_{j,s}{}' \psi_{b,s}^*(j)(-er_j)\psi_{a,s}(j). \tag{11}$$

Note that in the sum-over-state approach, the contribution to the spectrum is given by every dipole transition between the occupied state $|a\rangle$ and the unoccupied state $|b\rangle$ in the ground state. So the optical absorption spectrum is partially determined by the ground state of the system. Based on the extended SSH model, the optical absorption for pure or doped nanotubes can be computed. By comparing the results for pure nanotubes with that for the doped nanotubes, the effects of disorder on the optical absorption of the doped nanotubes could be observed.

We computed the averaged linear optical absorption $(|\alpha_{xx}|+|\alpha_{yy}|+|\alpha_{zz}|)/3$, and the results for a $j=15$ nanotube with different doped nitrogen atoms are shown in Fig. 9. The main observations are described as follows. First, it can be seen that for a pure nanotube, the optical absorption shows a slow ascension in small ω region [see Fig. 9(a)], but for doped nanotubes, where disorder plays a role, a quadric increase is found at infrared region [see Fig. 9(d)]. Secondly, in the absorption spectrum, a long tail can be seen for pure and slightly doped nanotubes, as shown in Figs. 9(a) and 9(b). From Figs. 4(a) and 4(b), we know these nanotubes are still in the regular regime. However, as shown in Figs. 9(c) and 9(d), with the increase of doped impurity atoms, the long tail in the optical absorption spectrum can be gradually suppressed and totally cleaned out in the disorder regime. For example, as shown in Fig. 9(d), an approximate ω^{-1} decay can be seen in the optical absorption for the doped nanotube with 13% (or 6.2%) nitrogen atoms. Thirdly, with the increase of doped impurity atoms, the peaks of optical absorption gradually shift towards the infrared region. Moreover, the peaks of the pure nanotube is depressed by the doped impurity atoms. As the increase of the doped impurity atoms,

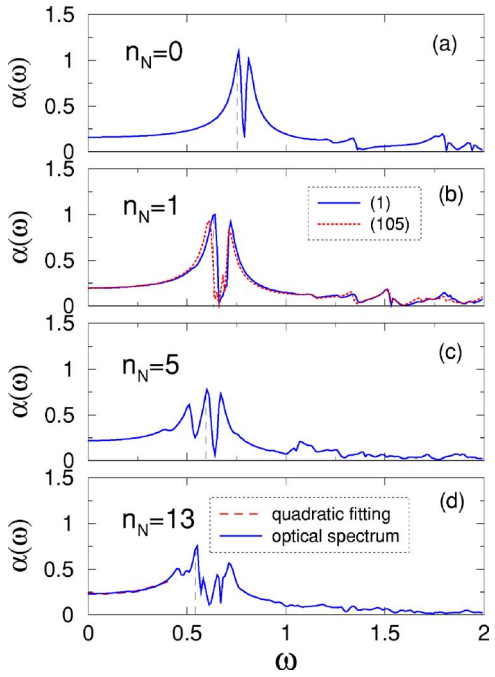

FIG. 9. (Color online) The linear polarizability of armchair nanotubes (in 10^{-20} esu). The total atoms are 210. In (b), the numbers in the bracket denote the positions of the doped nitrogen atoms. For (c) and (d), the doped nitrogen atoms are randomly distributed. In (d), the quadratic fitting is applied for the spectrum with $\omega < 0.4$. They match perfectly.

the peaks in the optical absorption spectrum gradually decrease. Experimentally, these phenomena can be used as the direct signature of disorder effect in heavily doped nanotubes.

We now provide a theoretical explanation for the observations shown in Fig. 9. Qualitatively speaking, peak values in the optical absorption spectrum of nanotubes are determined by the energy gap of the electronic structures. The larger the energy gap, the lower the peak. In the disorder regime, the statistics of energy level spacing satisfies the Wigner distribution, which implies that the nearest neighbor energy levels repel each other. Thus the gap between the HOMO and the LUMO has relatively large value. As the consequence, the peak values in the optical absorption spectrum of the heavily doped nanotubes are depressed. The above analysis is only a heuristic argument. In the following, a theoretical analysis is presented based on the random matrix theory.

In fact, random matrix has been successfully been employed to treat linear response theory,[34,35] which gives us confidence to treat the optical absorption for heavily doped nanotubes statistically. Taking into account the probability density of observing a level around each of points ϵ_a, ϵ_b, Eq. (10) could be rewritten by substituting two-level correlation function $R_2(\epsilon_a,\epsilon_b)=\langle d(E+\epsilon_a)d(E+\epsilon_b)\rangle$, where d stands for level density. In random matrix theory, the two-level correlation function R_2 consists of two elements. One is related to a product of two one-point functions, and the other is a minus two-level cluster function $Y_2(|\epsilon_a-\epsilon_b|)$. Since the first term only gives a trivial contribution independent of ω and could be neglected, we focus on the second term. Then the optical absorption formula can be written as

$$\alpha(\omega) \propto \sum_{a,b} \mu_{b,a}^2 \delta(\hbar\omega+\epsilon_a-\epsilon_b) Y_2(|\epsilon_a-\epsilon_b|). \tag{12}$$

Since the systems have enough energy levels, continuous parameters can be used to replace the discrete level summations. Then, following the spirit in linear response theory within the framework of random matrix,[34,35] the dipole matrix elements in above equation could be specified by an autocorrelation function of r. An identity for the general linear response cases concludes the Fourier transformation of autocorrelation functions with frequency $\hbar\omega=\epsilon_b-\epsilon_a$ could be used to replace the perturbation matrix element after ensemble average,[35,36] therefore its summation over ϵ_a,ϵ_b could be given by the integration of its Fourier transformation over the whole frequency region. After setting $\hbar\omega=\epsilon_b-\epsilon_a$ and temperature to zero $n_F(\epsilon_a)-n_F(\epsilon_a+\hbar\omega)=\theta(\epsilon_a)\theta(\hbar\omega-\epsilon_a)$, where n_F and θ denote the Fermi-Dirac distribution function and the step function, respectively, the energy integration results in a factor $\hbar\omega$. Putting together the different contributions, a compact formula for the optical absorption of disordered nanotubes could be obtained as

$$\alpha(\omega) \propto \hbar\omega Y_2(\hbar\omega)\bar{\mu}_{rr}(\omega), \tag{13}$$

where $\mu_{rr}(\omega)$ is the Fourier transformation of the time correlation function of $\mu_{rr}(\tau)$, which can be expressed as

$$\mu_{rr}(\omega) = \int d\tau \frac{e^{i\omega\tau}}{2\pi}\left[\lim_{T\to\infty}\frac{1}{T}\int_0^T dt r_j(t) r_j(t+\tau)\right]. \tag{14}$$

In Eq. (13), the bar over $\mu_{rr}(\omega)$ denotes the average. In a completely disordered system $\mu_{rr}(\tau)$ is a very complicated periodic function, its Fourier transformation, $\mu_{rr}(\omega)$ has small but rapid fluctuations around its mean value, which only raises some fine structures in optical absorption. Therefore, $\mu_{rr}(\omega)$ could be approximated by its mean value $\bar{\mu}_{rr}(\omega)$ [see Eq. (13)]. The two-level cluster function for Gaussian orthogonal ensemble is[37]

$$Y_2(\hbar\omega) = \left(\frac{\sin(\pi\hbar\omega)}{\pi\hbar\omega}\right)^2 + \frac{d}{d(\hbar\omega)}\left(\frac{\sin(\pi\hbar\omega)}{\pi\hbar\omega}\right)\int_{\hbar\omega}^{\infty}\frac{\sin(\pi t)}{\pi t}dt. \tag{15}$$

The asymptotic $\hbar\omega Y_2(\hbar\omega)$ yields a linear increase for very small $\hbar\omega$. In the small but intermediate $\hbar\omega$ region from 0.05 to 0.3, taking into account high order expansion terms, we still expect the optical absorption could follow quadric increase. On the other hand, in the limit $\omega\to\infty$, the two-level cluster function has the following asymptotic form:

$$Y_2(\hbar\omega) \simeq -(\pi\hbar\omega)^{-2} + (\pi\hbar\omega)^{-4}[3/2+\cos(2\pi\hbar\omega)], \tag{16}$$

which indicates that $\alpha(\omega)$ follows ω^{-1} decay as $\omega\to\infty$. These analyses are well consistent with our numerical observations in Fig. 9. Regarding the location of the peak optical absorption for doped nanotubes in disorder regime, it can also be

determined as following. At small and large ω ranges, the optical absorption seems to be very small. Since the fluctuations of $\bar{\mu}_{rr}(\omega)$ are very small, it still can be expected [see Eq. (13)] that in a completely disordered nanotube, the maximal optical absorption corresponds to the frequency which satisfies

$$\frac{\partial[\hbar\omega Y_2(\pi\hbar\omega)]}{\partial(\hbar\omega)} = 0. \tag{17}$$

Numerically solving Eq. (17), we found that the maximum peak in the optical absorption spectrum of nanotubes in totally disordered regime should be around normalized energy 0.5 eV. As shown in Fig. 9(d), the peak position in the spectrum of a disordered nanotube has moved to 0.55 eV, which approximately agrees with our analysis.

V. CONCLUDING REMARKS

In this paper, based on the extended SSH model, the electronic structures, the eigen wave functions, and the linear optical property of doped armchair nanotubes have been investigated. Our results show that the doped impurity atoms destroy the symmetry of pure nanotubes and thus strongly affect the Fermi energy gap and the eigen wave functions of the system. In heavily doped nanotubes, the statistics of the energy level spacing follow the Wigner distribution, and the entropies of eigen wave functions are large in the basis of pure system. These signatures clearly demonstrate that disorder plays by rules in heavily doped nanotubes. Furthermore, the relationship between the electronic structures and the linear optical absorptions for doped nanotubes have also been studied. The numerical simulations show that in the disorder regime the optical properties exhibit different characteristics from that of the pure nanotubes. For example, the optical absorptions are suppressed, and the maximum in the spectrum shifts toward the infrared direction. Using the random matrix theory, we carried out a theoretical analysis to reveal how disorder affects the optical properties of the doped nanotubes. The theoretical results are well consistent with the numerical observations. We hope that our results in the present study could be verified in the future experiments and applied in designing new microdevices.

ACKNOWLEDGMENTS

We thank J. Wang for helpful discussion. This work was supported by the Temasek Laboratories at the National University of Singapore. We specially thank the Department of Computational Science in the National University of Singapore for the use of computer facilities.

*Electronic address: tslgsg@nus.edu.sg

[1] M. Tabor, *Chaos and Integrability in Nonlinear Dynamics* (Wiley, New York, 1989).
[2] A. Ozorio de Almeida, *Hamiltonian Systems: Chaos and Quantization* (Cambridge University Press, Cambridge, 1988); L. E. Reichl, *The Transition to Chaos in Conservative Classical Systems: Quantum Manifestations* (Springer-Verlag, New York, 1992).
[3] F. Haake, *Quantum Signatures of Chaos* (Springer-Verlag, Berlin, 1991).
[4] P. W. Milonni, J. R. Ackerhalt, and H. W. Galbraith, Phys. Rev. Lett. **51**, 1108 (1983).
[5] A. Kujawski and M. Munz, Phys. Rev. A **35**, 5274 (1987).
[6] M. D. Crisp, Phys. Rev. A **43**, 2430 (1991).
[7] L. Bonci, R. Roncaglia, B. J. West, and P. Grigolini, Phys. Rev. Lett. **67**, 2593 (1991).
[8] A. Kudrolli, S. Sridhar, A. Pandey, and R. Ramaswamy, Phys. Rev. E **49**, R11 (1994).
[9] C. Dembowski, H.-D. Graf, A. Heine, R. Hofferbert, H. Rehfeld, and A. Richter, Phys. Rev. Lett. **84**, 867 (2000).
[10] A. Holle, J. Main, G. Weibusch, H. Rottke, and K. H. Welge, Phys. Rev. Lett. **61**, 161 (1988).
[11] J. Main, G. Weibusch, H. Rottke, and K. L. Welge, Comments At. Mol. Phys. **25**, 233 (1991).
[12] A. M. Chang, H. U. Baranger, L. N. Pfeiffer, and K. W. West, Phys. Rev. Lett. **73**, 2111 (1994).
[13] D. Weiss, M. L. Roukes, A. Menschig, P. Grambow, K. von Klitzing, and G. Weimann, Phys. Rev. Lett. **66**, 2790 (1991).
[14] J. Ma and R. K. Yuan, Phys. Rev. B **57**, 9343 (1998); N. Hamada, S. I. Sawada, and A. Oshiyama, Phys. Rev. Lett. **68**, 1579 (1992).
[15] T. Kato, T. Kodama, T. Shida, T. Nakagawa, Y. Matsui, S. Suzuki, H. Shiromaru, K. Yamauchi, and Y. Achiba, Chem. Phys. Lett. **180**, 446 (1991).
[16] T. Takahashi, S. Suzuki, T. Morikawa, H. Katayama-Yoshida, S. Hasegawa, H. Inokuchi, K. Seki, K. Kikuchi, S. Suzuki, K. Ikemoto, and Y. Achiba, Phys. Rev. Lett. **68**, 1232 (1992); P. A. Lane, L. S. Swanson, Q. X. Ni, J. Shinar, J. P. Engel, T. J. Barton, and L. Jones, *ibid.* **68**, 887 (1992).
[17] J. Dong, J. Jiang, J. Yu, Z. Wang, and D. Xing, Phys. Rev. B **52**, 9066 (1995); J. Dong, J. Jiang, J. Yu, Z. Wang, and D. Xing, *ibid.* **51**, 1997 (1995).
[18] R.-H. Xie and J. Jiang, Appl. Phys. Lett. **71**, 1029 (1997); R.-H. Xie, Chem. Phys. Lett. **310**, 379 (1999).
[19] K. Harigaya, Phys. Rev. B **45**, 13676 (1992); K. Harigaya, *ibid.* **48**, 2765 (1993).
[20] T. Guo, C. Jin, and R. E. Smalley, J. Phys. Chem. **95**, 4948 (1991); Y. Chai, T. Guo, C. Jin, R. E. Haufler, L. P. Felipe Chibante, J. Fure, L. Wang, J. Michael Alford, and R. E. Smalley, *ibid.* **95**, 7564 (1991).
[21] P. W. Anderson, Phys. Rev. **109**, 1492 (1958).
[22] K. Efetov, *Supersymmetry in Disorder and Chaos* (Cambridge University Press, Cambridge, 1996).
[23] T. Guhr, A. Muller-Groeling, and H. A. Weidenmuller, Phys. Rep. **299**, 189 (1998).
[24] N. Kurita, K. Kobayashi, H. Kumahora, and K. Tago, Phys. Rev. B **48**, 4850 (1993).
[25] N. Kurita, K. Kobayashi, H. Kumahora, K. Tago, and K. Ozawa, Chem. Phys. Lett. **198**, 95 (1992).
[26] T. A. Brody, J. Flores, J. B. French, P. A. Mello, A. Pandey, and

S. S. M. Wong, Rev. Mod. Phys. **53**, 385 (1981).
[27] R. U. Haq, A. Pandey, and O. Bohigas, Phys. Rev. Lett. **48**, 1086 (1982).
[28] L. Leviandier, M. Lombardi, R. Jost, and J. P. Pique, Phys. Rev. Lett. **56**, 2449 (1986).
[29] Y. Wang and L. T. Cheng, J. Phys. Chem. **96**, 1530 (1992).
[30] Q. Gong, Y. Sun, Z. Xia, Y. Zhou, Z. Gu, X. Zhou, and D. Qiang, J. Appl. Phys. **71**, 3025 (1992).
[31] W. J. Blau, H. J. Byrne, D. J. Cardin, T. J. Dennis, J. P. Hare, H. W. Kroto, R. Taylor, and D. R. M. Walton, Phys. Rev. Lett. **67**, 1423 (1991).
[32] Z. H. Kafafi, F. Bartoli, J. R. Lindle, and R. G. S. Pong, Phys. Rev. Lett. **68**, 2705 (1992).
[33] Z. Kafafi, J. R. Lindle, R. Pong, F. Bartoli, L. Lingg, and J. Milliken, Chem. Phys. Lett. **188**, 492 (1992); F. Kajzar, C. Taliani, R. Zamboni, S. Rossini, and R. Danieli, Synth. Met. **54**, 21 (1993); F. Kajzar, C. Taliani, R. Danieli, S. Rossini, and R. Zamboni, Phys. Rev. Lett. **73**, 1617 (1994); J. S. Meth, H. Vanherzeele, and Y. Wang, Chem. Phys. Lett. **197**, 26 (1992).
[34] A. Bulgac, G. Do Dang, and D. Kusnesov, Phys. Rev. E **54**, 3468 (1996).
[35] M. Hiller, D. Cohen, T. Geisel, and T. Kottos, Ann. Phys. (N.Y.) **321**, 1025 (2006).
[36] T. Prosen, Ann. Phys. (N.Y.) **235**, 115 (1994).
[37] M. L. Methta, *Random Matrices*, 2nd ed. (Academic, New York, 1991).